Population of Human Ventricular Cell Models Calibrated with *in vivo* Measurements unravels Ionic Mechanisms of Cardiac Alternans

Xin Zhou[1], Alfonso Bueno-Orovio[2], Michele Orini[3], Ben Hanson[3, 4], Martin Hayward[4], Peter Taggart[3, 4], Pier D Lambiase[3, 4], Kevin Burrage[1, 5], Blanca Rodriguez[1]

[1]Department of Computer Science, University of Oxford, Oxford, UK
[2]Oxford Centre for Collaborative Applied Mathematics, University of Oxford, Oxford, UK
[3]University College of London, London, UK
[4]The Heart Hospital, UCL Cardiovascular Institute, London, UK
[5]Queensland University of Technology, Queensland, Australia

Abstract

Cardiac alternans is an important risk factor in cardiac physiology, and is related to the initiation of arrhythmia in a number of pathological conditions. However, the mechanisms underlying the generation of alternans remain unclear. In this study, we used a population of computational models of human ventricular electrophysiology based on the O'Hara-Rudy dynamic model to explore the effect of 11 key factors experimentally reported to be related to cardiac alternans. In vivo experimental datasets obtained from patients undergoing cardiac surgery were used in the calibration of an in silico population of models. The calibrated models in the population were divided into two groups (Normal and Alternans) depending on the occurrence of the alternans. Our results showed that there were significant differences in the following 6 ionic currents between the two groups: the fast sodium current, the L-type calcium current, the rapid delayed rectifier potassium current, the sodium calcium exchanger current, the sarcoplasmic reticulum (SR) calcium release flux, and the SR calcium reuptake flux.

1. Introduction

Cardiac alternans is a repetitive beat-to-beat fluctuation between subsequent action potentials (APs), frequently observed in many pathophysiological conditions under significant metabolic stress and chrono-tropic stimulation [1]. Correspondingly, cardiac alternans has been regarded as an important risk factor for the genesis of ventricular arrhythmia and fibrillation [2].

Two major hypotheses have been developed to explain the generation of alternans in cardiac myocytes: the voltage-driven and the calcium-driven hypothesis. According to the voltage-driven hypothesis, the alternation in sarcolemmal currents can lead to fluctuations in membrane voltage and AP morphology, and then cause beat-to-beat fluctuations in intracellular Ca^{2+} concentration [2]. Modulation of sarcolemmal K^+ and Ca^{2+} currents has been reported to have a significant role on the stability of Ca^{2+} cycling and on the transition to stable alternans [2, 3]. Some other transmembrane proteins, such as the Na^+/Ca^{2+} exchanger and the Na^+/K^+ pump, may also play a role in the generation and maintenance of these alternans.

The calcium-driven hypothesis suggests alternation of intra-cellular Ca^{2+} concentration as the primary event, leading to changes in AP morphology and sarcolemmal currents [2]. The amount of Ca^{2+} release from the sarcoplasmic reticulum (SR) to initiate contraction must match the amount of Ca^{2+} reclaimed from the cytoplasm. Under this hypothesis, cardiac alternans occur when heart rate exceeds the capability of cardiac myocytes to recycle calcium. In this process, SR Ca^{2+} release by ryanodine receptors (RyRs) and re-uptake by sarco/endoplasmic reticulum Ca^{2+}-ATPase (SERCA) are the two major factors that affect the dynamic changes of intracellular Ca^{2+} concentration [2]. In addition, the Na^+/Ca^{2+} exchanger and the L-type calcium current may also be involved by affecting intracellular Ca^{2+} regulation.

The aim of this study is to use computational simulations to investigate the mechanisms underlying the generation of cardiac alternans in human ventricular cells based on *in vivo* electrophysiological recordings and a population-based approach.

2. Methods

2.1. Cell model population

In order to simulate the variability and uncertainty of

biological systems, one parameter set in a single model is insufficient. Instead, we base our analysis on a population of models of human ventricular electrophysiology utilizing the O'Hara *et al.* model [4]. Within this population, cell models share the same equations representing ionic current kinetics but different conductance values [5, 6].

The population of models is constructed by sampling the following 11 key parameters related to the generation of cardiac alternans: GNa (fast Na^+ channel conductance), PCa (Ca^{2+} channel permeability), GKs and GKr (conductances of the slow and rapid components of delayed K^+ rectifier current), GK1 (K^+ inward rectifier channel conductance), Gto (transient outward K^+ channel conductance), GNaL (late Na^+ channel conductance), GNaCa (Na^+/Ca^{2+} exchanger conductance), GNaK (Na^+/K^+ pump), Jrel (Ca^{2+} release via RyRs to myoplasm) and Jup (Ca^{2+} uptake via SERCA from the myoplasm).

2.2. Generation of model population

Due to the complexity of cardiac cell models and the large number of parameters, considering a fine discretization and every possible combination of parameter values is computationally intractable.

Latin hypercube sampling [7] was used in this study to generate scaling factors uniformly distributed between 0 and 2, which allows for an efficient and unbiased generation of parameter sets over large number of parameters [6]. Base model parameters in [4] were then multiplied by these scaling factors.

2.3. Data acquisition and signal analysis

In vivo information from 44 patients (9 female, 34 male) undergoing aortic valve replacement or coronary artery bypass grafting was used in this study for the calibration of the *in silico* population of models. Multielectrode activation and repolarization maps on the whole heart epicardial surface at multiple cycle lengths (CLs) were used to calculate activation-recovery intervals (ARIs) [8].

ARIs have been validated theoretically and experimentally as a measure of APD_{90} (AP duration to 90% repolarization); therefore, we used ARIs to constrain APD_{90} [9]. In order to exclude the effects of extreme values, 5^{th} and 95^{th} percentiles (Perc) of the total ARI data were calculated as APD_{90} thresholds, as shown in Table1.

Table 1. ARI thresholds for different cycle lengths (CL) used in the calibration of the models.

CL (ms)	600	550	500	450	400	350
ARI 5^{th}Perc (ms)	189	189	176	171	148	139
ARI 95^{th}Perc(ms)	366	337	305	285	259	230

2.4. Electrophysiological simulations

All numerical simulations were performed using the open source simulation software Chaste. Cellular models were stimulated for 1000 paces to guarantee steady-state conditions at each of the following CLs in a step protocol: 600, 500,450, 400, 350 and 300 ms.

3. Results

3.1. Calibration of models

10000 models were generated by varying 11 key ionic factors, as described in Methods. Any parameter sets that generated a model with unphysiological APD_{90}, resting and peak membrane potentials were excluded from the population. The physiological ranges for resting membrane potential were calculated from literature to be from -100 mV to -64 mV [10], whereas only models exhibiting peak membrane potentials greater than 0 mV were retained in the population. 2554 models were accepted in the final population after the experimental calibration (Figure 1).

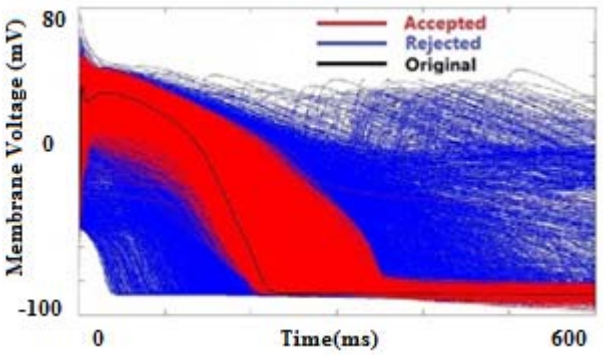

Figure 1. Population of models of human ventricular electrophysiology, paced at a CL=600 ms. Black: original O'Hara *et al.* model; blue: rejected models; red: accepted models after experimental calibration.

3.2. Analysis of cardiac alternans

The occurrence of APD and Ca^{2+} alternans was defined as a difference of greater than 5ms between APD_{80} (AP duration to 80% repolarization) or $CaTD_{80}$ (Ca^{2+} transient duration to 80% of repolarization) in the final steady-state APs of each pacing CL. For those models exhibiting an alternating behavior, no clear correlation was observed at any CL between the magnitudes of both types of cardiac alternans, with the magnitudes of CaTD alternans being significantly larger than the magnitudes of APD alternans (and vice versa) in a substantial portion of the model population (Figure 2).

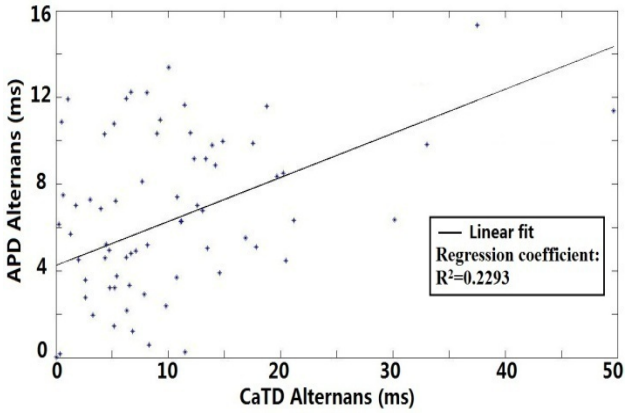

Figure 2. Analysis between APD and Ca^{2+} transient alternans at a CL=350 ms.

Human cellular models in the population were divided into two groups (Normal and Alternans), depending on the occurrence of alternans. Both Normal (non-alternating) and Alternans group models were distributed across the whole sampling range (Figure 3). Statistical analysis (Mann-Whitney U test) was used to compare the differences between both groups. For GNa, GCaL, GKr, GNaCa, Jrel and Jup, the differences were statistically significant (Figure 3). GNa and Jup were significantly smaller in the Alternans group, while GCaL, GKr, GNaCa, and Jrel were statistically larger in the Alternans group.

GNa, GNaCa, Jrel and Jup exhibited the most significant differences between the Normal and Alternans models groups (Figure 3). We compared the contribution of these four ionic factors on APD and CaTD alternans. The distributions of APD and CaTD alternans across parameter sampling ranges were very similar. Down-regulation of GNa and Jup facilitated the generation of both APD and CaTD alternans, similarly, up-regulation of GNaCa and Jrel promoted both APD and CaTD alternans (Figure 4).

4. Discussion and conclusions

In this study we built an experimentally-calibrated population of human ventricular electrophysiology models using the O'Hara *et al.* model and *in vivo* epicardial ARI values obtained in patients. Using the *in silico* human cell population, we detected the generation of APD and CaTD alternans and we quantified the contribution of ionic current conductances to alternans occurrence. Significant differences between GNa, GCaL, GKr, GNaCa, Jrel and Jup were observed in alternating vs. no alternating groups.

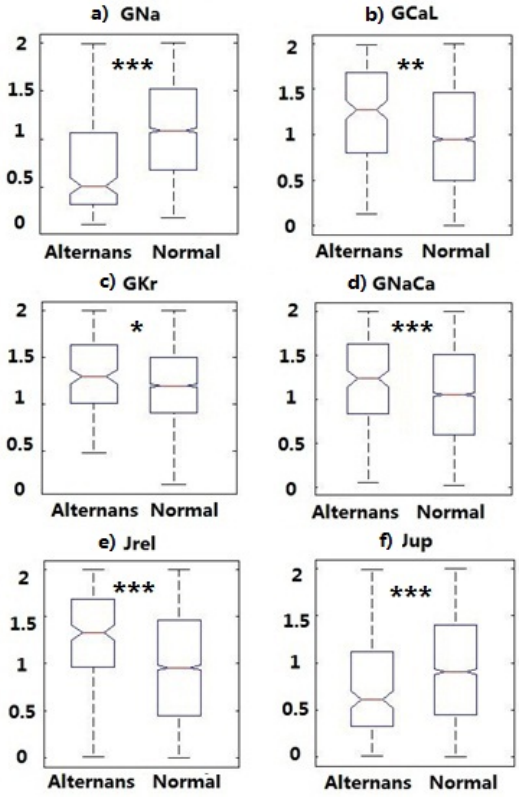

Figure 3. Ionic differences between alternans and normal groups. Central marks: distribution medians; box edges: 25th and 75th percentiles. Symbols indicate statistical differences: ***p<0.001; **p<0.01; *p<0.05.

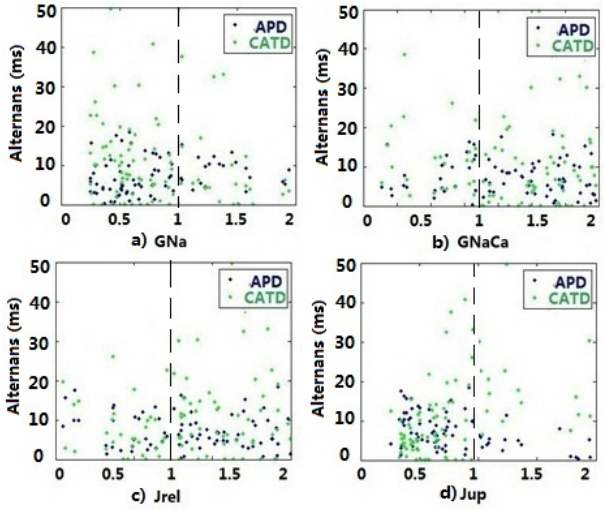

Figure 4. Relationship between two types of alternans and the distribution of parameters (CL=350 ms). Dashed lines: scaling factor=1 (original parameter).

Smaller GNa contributed to large APD and CaTD alternans at fast pacing rates. As GNa plays an important role in the depolarization period of the AP, modulation of

GNa may lead to alternans related to depolarization rather than just at the repolarization stage. Importantly, as shown in Fig. 5, data from high density mapping of the *in vivo* human heart show that in certain cases APD and depolarization alternans can occur simultaneously.

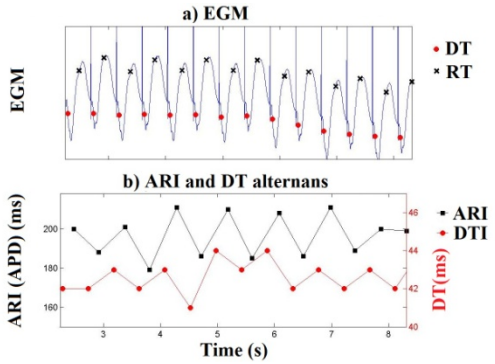

Figure 5: (a) Epicardial electrogram (EGM). Markers represent depolarization (DT) and repolarization (RT) time. (b) APD and depolarization (DT interval, DTI) alternans occur simultaneously.

The rest of parameters, however, may mainly affect alternans generation during the repolarization process. Insufficient SR Ca^{2+} re-uptake or excess of SR Ca^{2+} release in cardiac myocytes may cause an increase of the cytosolic Ca^{2+} concentration, and therefore disturb the SR Ca^{2+}-induced/Ca^{2+}-release mechanism, leading to Ca^{2+} alternans. It has also been found experimentally that over-expression of SR Ca^{2+} re-uptake can facilitate resistance to APD alternans [11]. The Na^{+}/Ca^{2+} exchanger and the L-type Ca^{2+} current may also be involved in this process by affecting the intracellular Ca^{2+} cycle. GKr may play a role in this process by affecting the repolarization duration: a larger GKr will decrease the time for Ca^{2+} cycle recovery and therefore enable alternans generation.

The results in this study were based on the initial analysis of the *in vivo* data from 44 individuals. Currently, we used the overall ARI ranges from all patients to calibrate the APD_{90} of the cellular models. Future work may extend this approach by developing further subpopulations based on gender, age and the condition of patients. In this study, physiological resting and peak membrane potentials were also included in the calibration; additional physiological information may be incorporated into this process in the future to make the results closer to physiological observations. Tissue level simulations may also be considered in the analysis of alternans in future studies.

Acknowledgements

X.Z. was supported by China Scholarship Council and EPSRC-funded Systems Biology Doctoral Training Centre program. A.B.O. was supported by Award No. KUK-C1-013-04, made by King Abdullah University of Science and Technology (KAUST). P.L. was supported by MRC grant number G901089. B.R. holds Medical Research Council Career Development, Industrial Partnership and Centenary Awards. The authors would like to acknowledge John Walmsley, Oliver J. Britton, Dr Jonathan Cooper, Chaste team and the Oxford Supercomputing Centre (OSC) for their help in this work.

References

[1] Hüser J, et al. Functional coupling between glycolysis and excitation-contraction coupling underlies alternans in cat heart cells. J Physiol 2000;524:795–806.

[2] Merchant FM, et al. Role of substrate and triggers in the genesis of cardiac alternans, from the myocyte to the whole heart: implications for therapy. Circulation 2012;125:539–549.

[3] Armoundas AA. Mechanism of abnormal sarcoplasmic reticulum calcium release in canine left-ventricular myocytes results in cellular alternans. IEEE Trans Biomed Eng 2009;56:220–228.

[4] O'Hara T, et al. Simulation of the undiseased human cardiac ventricular action potential: model formulation and experimental validation. PLoS Comput Biol 2011;7:e1002061.

[5] Walmsley J, et al. mRNA expression levels in failing human hearts predict cellular electrophysiological remodeling: a population-based simulation study. PLoS ONE 2013;8:e56359.

[6] Britton OJ, et al. Experimentally-calibrated population of models predicts and explains inter-subject variability in cardiac cellular electrophysiology. Proc Natl Acad Sci USA 2013;110: E2098–2105.

[7] Mckay MD, et al. A comparison of three methods for selecting values of input variables in the analysis of output from a computer code. Technometrics 1979;21:239–245.

[8] Nash MP, et al. Evidence for multiple mechanisms in human ventricular fibrillation. Circulation 2006;114:536–542.

[9] Bueno-Orovio A, et al. In vivo human left-to-right ventricular differences in rate adaptation transiently increase pro-arrhythmic risk following rate acceleration. PLoS ONE 2012;7:e52234.

[10] Li G, et al. Ionic current abnormalities associated with prolonged action potentials in cardiomyocytes from diseased human right ventricles. Heart Rhythm 2004;4: 460–468

[11] Cutler MJ, et al. Targeted SERCA2a gene expression identifies molecular mechanism and therapeutic target for arrhythmogenic cardiac alternans. Circ Arrhythm Electrophysiol 2009; 2: 686–694.

Address for correspondence.

Xin Zhou
Department of Computer Science, University of Oxford
Wolfson Building, Parks Road, Oxford OX1 3QD, UK